Soft Matter

Cite this: *Soft Matter*, 2012, **8**, 11180

www.rsc.org/softmatter

PAPER

Spreading and retraction dynamics of a dye doped smectic liquid crystal domain at the air–water interface†

P. Viswanath,*[ab] K. A. Suresh[a] and Bharat Kumar[b]

Received 12th June 2012, Accepted 22nd August 2012
DOI: 10.1039/c2sm26358k

We have studied the spreading and retraction dynamics of a dye doped smectic multilayer domain in the collapsed state of a Langmuir monolayer at the air–water interface. We find that the domain undergoes shearing when excited with an appropriate wavelength in the epifluorescence setting of the microscope. The shearing leads to displacement of the stack of layers and results in asymmetric spreading of the domain. Eventually, due to line tension, the domain transforms into a circular shape. Here, the domain area was about twice that of the initial area. Under reflection setting of the microscope, with white light, we observe that the domain retracts to a smaller area. During the course of retraction, we find successive generation and evolution of edge dislocation loops leading to thickening of the domain. Our analysis on the variation of the normalized area of the domain with time yields different characteristic time constants for spreading and retraction. The spreading and retraction of the domain can be understood by invoking changes in interfacial tension due to photobleached surface active products and the depletion of photobleached products, respectively.

1 Introduction

The spreading of a liquid drop over a liquid subphase has drawn a lot of attention due to its direct relevance in oil recovery, spillage, emulsion stability, foaming and anti-foaming agents.[1] There have been many studies on the dynamics of spreading of a liquid drop over a liquid subphase.[2–5] A few studies have also concentrated on the spreading and retraction dynamics of a drop of surfactant solution deposited over liquid subphase where the surfactant, its diffusion and solvent evaporation play a crucial role in dictating the dynamics.[6,7] There is also a report on the spreading and retraction of a drop aided by an interfacial reaction.[8] In the literature, studies on liquid crystal (LC) domain over a liquid subphase have focused on the structure of LC domains,[9,10] optical textures[11,12] and line tension measurements.[10,13] However, spreading and retraction dynamics of a LC domain in equilibrium with a thin film at the air–water (A–W) interface have not drawn much attention. In contrast to the spreading dynamics of an isotropic droplet, the molecular ordering in the LC phase, its viscoelasticity and anchoring at the interface should lead to interesting dynamics. These should have implications in polymer dispersed and other liquid crystal displays.[14] In this article, we report the spreading and retraction dynamics of a smectic (Sm) LC domain doped with a fluorescent dye at the A–W interface.

2 Experimental

The LC material, 4′-octyl-4-biphenylcarbonitrile, 8CB (Aldrich) doped with 1% molar concentration of an amphiphilic fluorescent dye, 4-(hexadecylamino)-7-nitrobenz-2-oxa-1,3-diazole (Molecular Probes) was dissolved in chloroform (1 mg ml^{-1}). Using a Hamilton micro-syringe, the solution was added drop by drop over the water subphase (Millipore, resistivity >18.2 MΩ cm, TOC <5 ppb) in a Langmuir trough at 25 °C. After equilibrating for 15 minutes, the monolayer was symmetrically compressed using two barriers at a rate of 0.02 $Å^2$ per molecule per s. The surface pressure (π)–area per molecule (A_m) isotherm of 8CB (Fig. 1) exhibited the sequence: a coexisting gas + low density liquid (L_1) phase, an L_1 phase and a collapsed state. The collapsed state exhibited a coexisting L_1 + trilayer phase which on further compression transformed into a trilayer + multilayer (stack of interdigitated bilayers on top of a monolayer) phase. The isotherm of 8CB molecules and its phase sequence at the A–W interface are in agreement with those reported in the literature.[9,15,16] The addition of the dye had negligible effect on the nature of the isotherm. Polarizing microscope studies on the multilayer domains have shown a smectic A-like ordering with homeotropic alignment.[11] We have carried out the spreading and retraction studies on the multilayer domains in the collapsed state at an A_m of 8 $Å^2$ per molecule.

The schematic diagram of the experimental setup is shown in Fig. 2. A Leitz Metalux 3 microscope (25× objective, 0.4 NA)

[a]*Centre for Soft Matter Research, Jalahalli, Bangalore, 560 013, India. E-mail: viswanath@csmr.res.in; Fax: +91 80 2838 2044; Tel: +91 80 2838 2924*
[b]*Raman Research Institute, Sadashivanagar, Bangalore, 560 080, India*

† Electronic supplementary information (ESI) available: Movie on spreading and retraction of the dye doped smectic liquid crystal domain at the air–water interface. See DOI: 10.1039/c2sm26358k

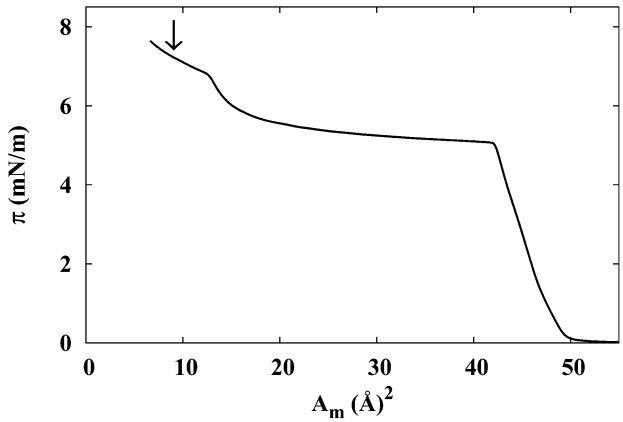

Fig. 1 Surface pressure (π)–area per molecule (A_m) isotherm of 8CB at 25 °C. The arrow indicates the A_m (8 Å^2 per molecule) at which the spreading and retraction experiments were carried out.

equipped with a CCD camera (DXC 390P, Sony) was used for observation of the Sm multilayer domains at the A–W interface at normal incidence. The pixels of the CCD camera were square and hence did not introduce any distortion in the image. The microscope can be adapted to view the domains either in reflection or epifluorescence setting (Fig. 2). The images of the domain were grabbed using a frame grabber (PCI 1411, National Instruments) at a rate of one frame per second and were processed using ImageJ.[17] The trough was shielded to minimize the drift of the domains arising due to air currents. The following procedure was adopted to study the Sm multilayer domain under the microscope: a domain in the unperturbed state was observed in reflection setting (100 W Hg lamp, white light). Then, we changed to epifluorescence setting (by introducing appropriate dichroic filters, ~450 nm, for excitation of dye, and ~530 nm, for fluorescence emission, in the path of the white light) to activate and observe the dye doped domain. Here we find spontaneous spreading of the domain. When the area of the domain attains its maximum size, we return to reflection setting.

An imaging ellipsometer (EP3-SWIE, Accurion) with a laser of wavelength 532 nm was used for measuring the thickness of the coexisting Sm multilayer domains at the A–W interface.

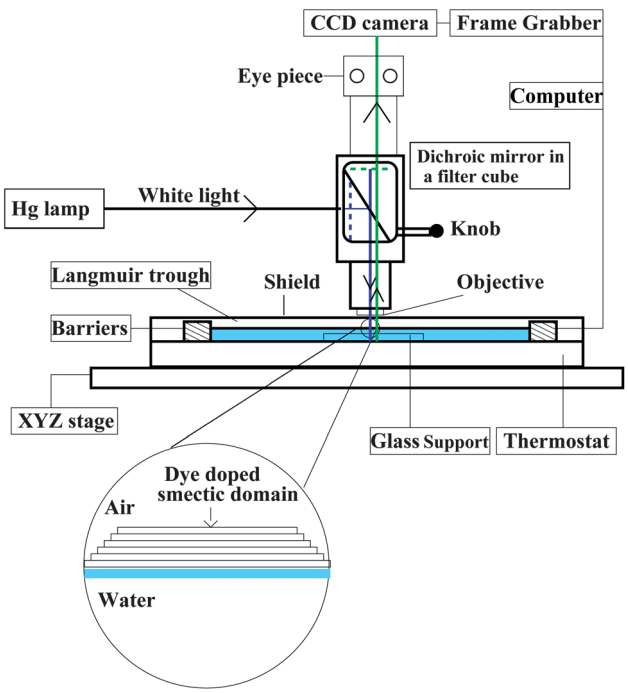

Fig. 2 Schematic diagram of the experimental setup used for studying the spreading and retraction dynamics of the dye doped smectic domain at the air–water interface. The knob shown in the figure can be flipped to change between epifluorescence and reflection settings. In the former case, a dichroic mirror facilitates selection of the excitation wavelength at 450 nm and emission at 530 nm. In the latter case, the dichroic mirror is replaced by a partially reflecting mirror.

3 Results and discussion

In the reflection setting, each smectic domain exhibited a characteristic color depending on its thickness. This is due to interference between the Sm–air and Sm–water interfaces.[11] The uniform color over the area of the domain indicated its flatness (Fig. 3(a)). In the epifluorescence setting, the domain spreads with time as shown in Fig. 3(b)–(d). Interestingly, during this process, we find shearing of stacks of layers from the domain. As a result, the domain changes to asymmetric shape (Fig. 3(c)). Further, the domain transforms into a circular shape due to line tension. Here, the area of the domain (Fig. 3(d)) was almost twice that of the initial domain (Fig. 3(a)). The Sm domain, which was initially bright (Fig. 3(b)), tends to fade with time during spreading (Fig. 3(c) and (d)). The spreading behavior of the

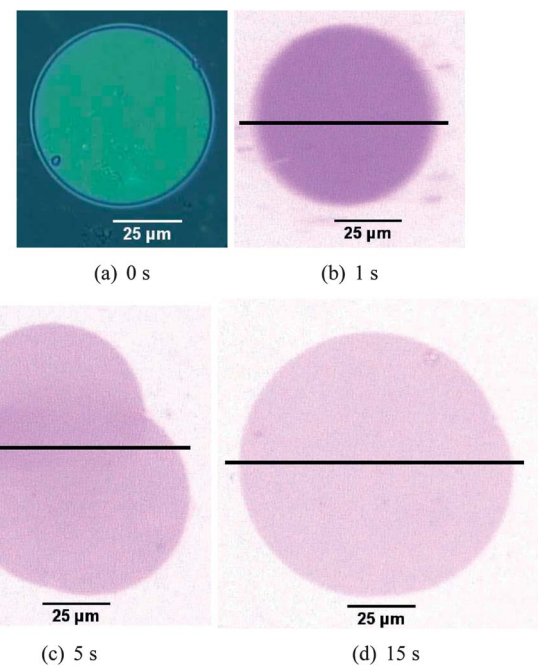

Fig. 3 (a) Dye doped smectic domain in reflection setting (illuminated with white light) of the microscope at the air–water interface. (b) The same domain in epifluorescence setting (excitation 450 nm and fluorescence 530 nm). (c and d) show the spreading of the domain in epifluorescence setting. Here the images (b)–(d) are contrast inverted for better clarity.

domain can also be seen in reflection setting at a higher dye concentration (>5%). However, the epifluorescence setting was far more efficient since we could selectively choose the excitation wavelength which facilitated spreading at low dye concentration (~1%). The fluorescent intensity profiles obtained across the domains at different instants of time are shown in Fig. 4(a). The profiles corresponding to 1 s and 15 s indicated a homogeneous distribution of the dye within the Sm domain. The profiles show a reduction in the fluorescence intensity during spreading. As the area of the domain increases during spreading, the fluorophore density reduces leading to a decrease in intensity. The photobleaching also results in a decrease in intensity. The peak fluorescent intensity was determined by averaging the intensity (for a length of about 5 μm) at the centre of the domain. Fig. 4(b) shows the variation of peak fluorescent intensity with time. It was fitted to a relationship of the type, $I_f = a_f\exp(-t/\tau_f) + b_f$. The fitting yielded the values, $a_f = 60.5 \pm 2.0$, $b_f = 20.7 \pm 1.8$ and the characteristic time constant, $\tau_f = 4.4 \pm 0.4$ s.

When the domain area reaches saturation, we change over to reflection setting (white light, where the dye is least excited). We refer to this situation as the post-bleached regime. In this regime, the domain starts retracting to a smaller area (Fig. 5). Surprisingly, the decrease in area of the domain was accompanied by successive generation and evolution of loops originating from a point. This is shown in Fig. 5(b) and (c). A dust particle which was located at the periphery of the domain (Fig. 5(a)) acted as a nucleus for the generation of loops. The evolution of loops was

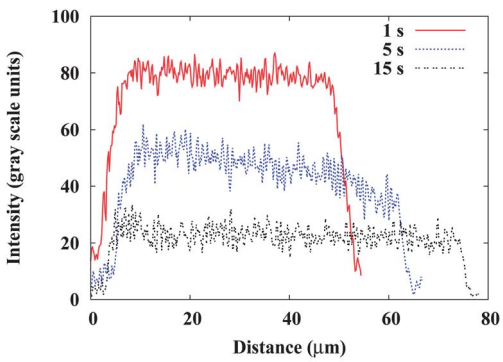

(a)

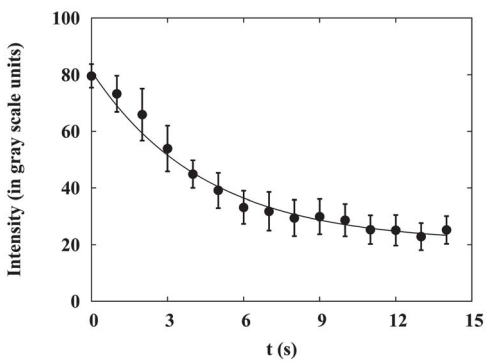

(b)

Fig. 4 (a) Intensity profiles corresponding to the line drawn across the domains in Fig. 3(b)–(d). (b) Variation of the peak fluorescent intensity with time during spreading of the domain. The data were fitted to a relationship of the type, $I_f = a_f\exp(-t/\tau_f) + b_f$.

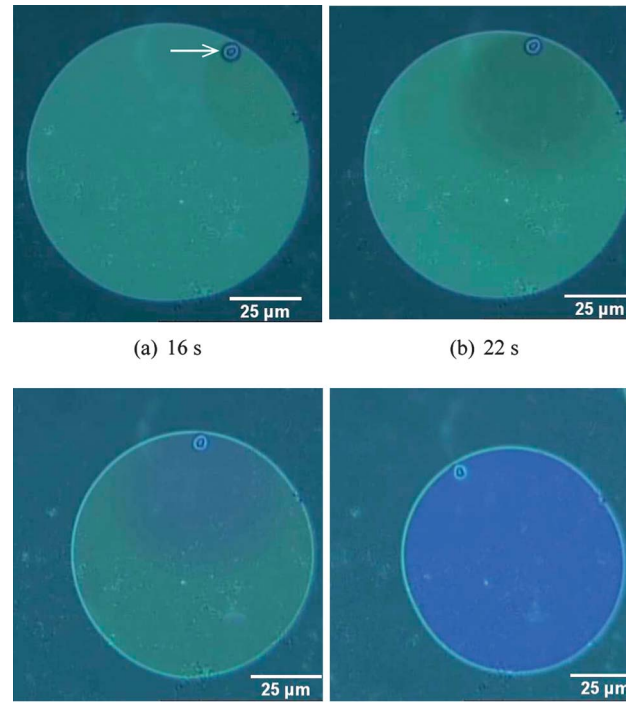

(a) 16 s (b) 22 s

(c) 34 s (d) 75 s

Fig. 5 Microscope images of the photobleached smectic domain in reflection setting (illuminated with white light) during retraction at the air–water interface. (a)–(d) show the domain at different instants of time. Evolution of loops within a domain leads to changes in colors. A dust particle (shown by the arrow in (a)) acts as a nucleus for the generation of loops. In (d), the domain is slightly distorted due to a local inhomogeneity on the substrate.

accompanied by a change in interference colors of the Sm domain. During this process, we could observe 16 loops originating from the nucleus one after another. Typically, at about 75 seconds, the area of the domain attained a steady state (Fig. 5(d)). The entire sequence of spreading and retraction of the domain is shown as a movie in the ESI.† The area remained unchanged even up to 15 minutes of observation in reflection setting. Also, the area at this stage was 1.4 times that of the initial area.

The change in the normalized area (A_t/A_0) of the Sm domain with time, t, during spreading and retraction is shown in Fig. 6. We have fitted the spreading and retraction data to a relationship of the type, $A_t/A_0 = a_j\exp(-t/\tau_j) + b_j$, where a, b are constants and τ is the characteristic time constant. The suffix, j refers to either spreading (s) or retraction (r). Fitting the data up to 15 s yields $a_s = -1.7 \pm 0.1$, $b_s = 2.1 \pm 0.03$ and $\tau_s = 2.3 \pm 0.2$ s. We find that the characteristic time for the fluorescent decay (τ_f) is about twice that of the time constant (τ_s) for the spreading of the domain. For the case of retraction (after 15 s), the values obtained by fitting were $a_r = 2.7 \pm 0.1$, $b_r = 1.40 \pm 0.01$, and $\tau_r = 14.5 \pm 0.4$ s. The time constant for spreading of the domain is smaller than that obtained for retraction.

During spreading, the stack of layers gets sheared from the domain. The following procedure was adopted to measure the displacement of the stacks. The sheared front was fitted to a circle and its origin (x_0, y_0) was determined. As the front moved, this

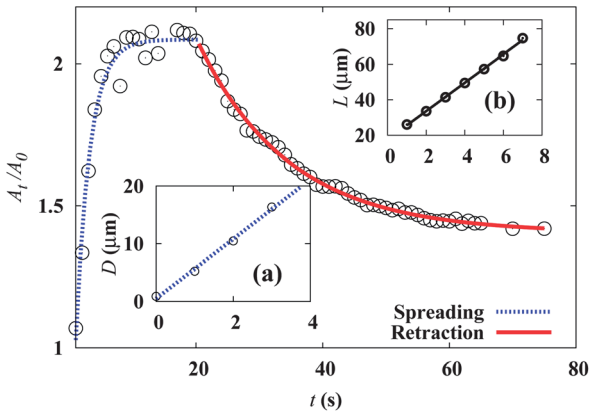

Fig. 6 Normalized area (A_t/A_0) of the dye doped smectic domain with time, t, during spreading (up to 15 s, in epifluorescence setting) and retraction (after 15 s, in reflection setting). The data were fitted to a relationship of the type, $A_t/A_0 = a_j\exp(-t/\tau_j) + b_j$. The inset (a) shows the displacement of the stack of layers, D, with t during spreading. The slope yields a velocity of 5.2 ± 0.2 μm s^{-1}. The inset (b) shows the displacement (the farthest point of the loop from the nucleus), L, with t of a typical loop within a domain during retraction. The slope yields a velocity of 8.0 ± 0.1 μm s^{-1}.

origin was tracked with time. The displacement, D, was calculated using the expression, $D = \sqrt{(x-x_0)^2 + (y-y_0)^2}$ which is shown as an inset (a) in Fig. 6. Fitting the data to a straight line yields a velocity of 5.2 ± 0.2 μm s^{-1}. During retraction, the displacement of a typical loop within a domain was tracked with time. The displacement, L, was measured from the nucleus to the farthest point of the loop. This is also shown as an inset (b) in Fig. 6. The slope yields a velocity of 8.0 ± 0.1 μm s^{-1}. These parameters depend on the photoresponse of the dye, its effect on the line tension and viscoelasticity of 8CB.

Géminard *et al.* have studied the layer thinning dynamics induced by temperature in a freestanding Sm film of 8CB.[18,19] In their case, the thinning of the film is accompanied by the formation of an edge dislocation loop. The thickness of the film reported in their experiment was much larger (~300 nm). The typical domain thickness in our experiment was about 50 nm. Géminard *et al.* find a constant velocity (~1 μm s^{-1}) for the loop when the radius of the loop was greater than the critical radius. We also find a constant velocity of 8 μm s^{-1} (inset (b) in Fig. 6). In comparison, it indicates that the radius of the loop is greater than the critical radius. In the light of their results and also from our studies, we infer that the loops generated during thickening of the domain are indeed edge dislocation loops. It is known that the creation of a dislocation depends on its energy which is proportional to the square of its Burgers vector. A dislocation of least energy will have a Burgers vector of one lattice unit.

Bougrioua *et al.* have reported light induced layer by layer thickening of a photosensitive liquid crystal membrane which is dependent on illumination conditions.[20] Unlike the edge dislocation loop, they find that the newly formed layers during the thickening process do not cover up to the meniscus size. This indicates a different mechanism for the evolution of layers during thickening.

To ascertain the thickness independently, the domains were observed at the same A_m (8 Å^2 per molecule) under an imaging ellipsometer. Here, we have deliberately chosen a region of the film at the A–W interface where many multilayer domains coexist. On the other hand, for the spreading dynamics, we studied an isolated domain in order to avoid domain–domain interactions. We have mapped the ellipsometric parameter, Δ (phase shift) for the Sm domains (Fig. 7). The domains were assumed to be in the homeotropic alignment. The values of the refractive indices of the ordinary (1.525) and the extra-ordinary (1.682) rays were obtained from the literature.[16,21] Using the EP4 modeling software, the thicknesses of some typical domains obtained were 69.3 ± 0.2 nm, 74.8 ± 0.2 nm and 44.2 ± 0.2 nm (Fig. 7). These values have the same order of magnitude as that of the domain on which the spreading and retraction observations were carried out. The phase shift corresponding to the background indicated a trilayer agreeing with an earlier report.[15]

The spreading coefficient (S) of an isotropic liquid on water subphase can be written as,[1,2]

$$S = \sigma_{\text{water–air}} - \sigma_{\text{liquid–water}} - \sigma_{\text{liquid–air}}$$

where $\sigma_{\text{water–air}}$, $\sigma_{\text{liquid–air}}$ are the surface tension of water and liquid, respectively. $\sigma_{\text{liquid–water}}$ is the interfacial tension of liquid with respect to water. The liquid spreads and completely wets if S is >0 or partially wets (dewets) to form a lens if S is <0. In the liquid crystalline phase, apart from the surface tension components, the elastic contribution[12,22] to S is given by, $K\theta^2/2h$, where K is the Frank elastic constant, θ is the angle made by the director with respect to surface normal and h is the thickness of the domain. For a typical domain with $K = 5.2 \times 10^{-12}$ N,[19] $\theta = \pi/2$ and $h = 50$ nm, the elastic contribution turns out to be 0.1 mN m^{-1}. However, in the extreme case of a very thin film like a trilayer, the elastic contribution may be significant (~3.5 mN m^{-1}). From the literature, using the values of surface tension, $\sigma_{\text{Sm–air},0} = 29.6$ mN m^{-1} (ref. 23) $\sigma_{\text{Sm–water},0} = 38$ mN m^{-1} (ref. 10) and the elastic contribution in S, we get, $S_{\text{initial}} = 72.8 - 29.6 - 38 - 0.1 = 5.1 > 0$ leading to spreading. In the collapsed state (at 8 Å^2 per molecule), the surface pressure is about 7 mN m^{-1}. This leads to, $S_{\text{final}} = S_{\text{initial}} - \pi \sim -2$ indicating dewetting of the multilayer domain.[24]

Van Nierop *et al.* have reported spreading and recoil dynamics of a drop of oil containing oleic acid deposited on an aqueous sodium hydroxide solution.[8] The radius of the droplet was then monitored with time. They find a power law dependence of the radius of the drop with time during spreading and also during

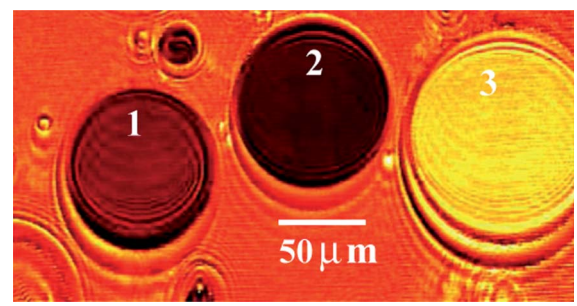

Fig. 7 The phase shift (Δ) map of the smectic domains at the air–water interface, obtained under an imaging ellipsometer (EP3-SWIE). Different colors indicate different phase shifts. For the domains labelled, 1, 2 and 3, the thicknesses obtained were 69.3 nm, 74.8 nm and 44.2 nm, respectively.

retraction. The exponents obtained were found to depend on the concentration of the reactants. In our experiment, the Sm LC domain was in equilibrium with a thin trilayer background where the photobleaching facilitates spreading of the domain. Extending the arguments of van Nierop *et al.* for a first order reaction with a rate constant k, we obtain, $\sigma_{l}(t) = \sigma_{l,\infty} - (\sigma_{l,\infty} - \sigma_{l,0})\exp(-kt)$ where the suffix l refers to either σ_{Sm-air} or $\sigma_{Sm-water}$. It is clear from the above expression that the sign of S can be positive or negative driving either spreading or retraction, respectively.

We can understand the spreading and retraction behavior of the Sm domain as follows: in epifluorescence setting, the fluorescent dye in the Sm domain gets partially photobleached during excitation (450 nm). In the presence of light and oxygen (in the air), the fluorophore decomposes and yields photobleached products.[25] These products act as surface active agents which diffuse and get adsorbed at the Sm–water interface. This results in a dynamic change in the surface tension of Sm phase, $\sigma_{Sm-air}(t)$ and the interfacial tension of Sm phase with respect to water, $\sigma_{Sm-water}(t)$ leading to an increase in S. Also, the illumination of the domain from above sets up a gradient in the concentration of surfactant. The resulting gradient in the surface tension induces shear stress in the Sm domain. This is similar to the Marangoni spreading well known in surfactant enriched liquid drop over a liquid film.[26] In our case, since the domain has a layered structure, under shear stress, it spreads asymmetrically. Thereafter, the bleached products diffuse to the subphase resulting in decrease of S. This causes dewetting and hence retraction of the domain.

We have also studied the Sm films doped with the dye transferred onto a glass substrate at an A_m of 8 Å^2 per molecule using the horizontal transfer method. Though the overall fluorescence tends to decrease with time, the multiple heterogeneities of the substrate led to pinning of the boundary, inhibiting spreading of the domain. These studies indicated that the weak anchoring of the Sm domain on the water surface plays a crucial role. The water subphase serves as a medium in transporting and dispersing the insoluble photobleached surfactants thereby facilitating the spreading dynamics. In addition, the fluorescent dopant concentration, photobleaching quantum yield of the fluorophore, intensity of the excitation radiation and the viscosity ratio of the subphase to the Sm domain influence the spreading and retraction behavior.

4 Conclusions

The Sm domain doped with a fluorescent dye undergoes photobleaching in the epifluorescence setting at the A–W interface. The photobleaching modifies the Sm–air and Sm–water interfacial tensions. The domain undergoes shearing leading to the displacement of a stack of layers. This results in spreading of the domain to a larger area and the domain thins down. In the post-bleached regime, in reflection setting, the domain retracts. During retraction, edge dislocation loops generated successively from a nucleus lead to an increase in thickness of the domain. The characteristic time constant obtained for spreading is less than that obtained for retraction. These studies have relevance to liquid crystal emulsions[27] and dispersions.[14] The spreading and retraction of the smectic domain on a thin film of trilayer at the air–water interface mimic the spreading of pulmonary lung surfactant over the thick mucous layer encountered in the respiratory distress syndrome.[28]

Acknowledgements

The authors thank K.R. Vinaya Kumar for his assistance in ellipsometry measurements and Prof. G.S. Ranganath for useful discussions. A part of this work was carried out under INSA-HAS bilateral scientific project (2010–2012). We also thank the Referees for useful suggestions.

References

1 D. Bonn, J. Eggers, J. Indekeu, J. Meunier and E. Rolley, *Rev. Mod. Phys.*, 2009, **81**, 739–805.
2 A. B. Afsar-Siddiqui, P. F. Luckham and O. K. Matar, *Adv. Colloid Interface Sci.*, 2003, **106**, 183–236.
3 O. K. Matar and R. V. Craster, *Soft Matter*, 2009, **5**, 3801–3809.
4 V. Bergeron and D. Langevin, *Phys. Rev. Lett.*, 1996, **76**, 3152–3155.
5 D. W. Fallest, A. M. Lichtenberger, C. J. Fox and K. E. Daniels, *New J. Phys.*, 2010, **12**, 073029.
6 T. F. Svitova, R. M. Hill and C. J. Radke, *Langmuir*, 2001, **17**, 335–348.
7 D. Chowdhury, S. P. Sarkar, D. Kalita, T. K. Sarma, A. Paul and A. Chattopadhyay, *Langmuir*, 2004, **20**, 1251–1257.
8 E. A. van Nierop, A. Ajdari and H. A. Stone, *Phys. Fluids*, 2006, **18**, 038105.
9 M. C. Friedenberg, G. G. Fuller, C. W. Frank and C. R. Robertson, *Langmuir*, 1994, **10**, 1251–1256.
10 L. Zou, J. Wang, P. Basnet and E. K. Mann, *Phys. Rev. E: Stat., Nonlinear, Soft Matter Phys.*, 2007, **76**, 031602.
11 K. A. Suresh and A. Bhattacharyya, *Langmuir*, 1997, **13**, 1377–1380.
12 U. Delabre, C. Richard and A. M. Cazabat, *J. Phys. Chem. B*, 2009, **113**, 3647–3652.
13 U. Delabre, C. Richard, J. Meunier and A. M. Cazabat, *Europhys. Lett.*, 2008, **83**, 66004.
14 P. S. Drzaic, *Liquid Crystal Dispersions*, World Scientific Publishing Ltd, Singapore, 1998.
15 J. Xue, C. S. Jung and M. W. Kim, *Phys. Rev. Lett.*, 1992, **69**, 474.
16 M. N. G. de Mul and J. A. Mann, *Langmuir*, 1998, **14**, 2455–2466.
17 W. S. Rasband, *ImageJ*, NIH, Bethesda, Maryland, USA, 1997–2009, http://rsb.info.nih.gov/ij/.
18 J. C. Géminard, R. Holyst and P. Oswald, *Phys. Rev. Lett.*, 1997, **78**, 1924–1927.
19 A. Zywocinski, F. Picano, P. Oswald and J. Géminard, *Phys. Rev. E: Stat. Phys., Plasmas, Fluids, Relat. Interdiscip. Top.*, 2000, **62**, 8133–8140.
20 F. Bougrioua, P. Cluzeau, P. Dolganov, G. Joly, H. T. Nguyen and V. Dolganov, *Phys. Rev. Lett.*, 2005, **95**, 027802.
21 P. P. Karat and N. V. Madhusudana, *Mol. Cryst. Liq. Cryst.*, 1976, **36**, 51–64.
22 A. D. Rey, *Langmuir*, 2001, **17**, 1922–1927.
23 T. B. M. Tintaru, R. Moldovan and S. Frunza, *Liq. Cryst.*, 2000, **28**, 793–797.
24 U. Delabre, C. Richard and A. M. Cazabat, *J. Phys.: Condens. Matter*, 2009, **21**, 464129.
25 D. Axelrod, D. E. Koppel, J. Schlessinger, E. Elson and W. W. Webb, *Biophys. J.*, 1976, **16**, 1055–1069.
26 D. A. Edwards, H. Brenner and D. T. Wasan, *Interfacial Transport Processes and Rheology*, Butterworth-Heinemann, 1991.
27 Y. Iwashita, S. Herminghaus, R. Seemann and C. Bahr, *Phys. Rev. E: Stat., Nonlinear, Soft Matter Phys.*, 2010, **81**, 051709.
28 J. A. Zasadzinski, J. Ding, H. E. Warriner, F. Bringezu and A. J. Waring, *Curr. Opin. Colloid Interface Sci.*, 2001, **6**, 506–513.